The Degrees of Freedom of Wireless Networks Via Cut-Set Integrals

Massimo Franceschetti, *Member, IEEE*, Marco Donald Migliore, *Member, IEEE*, Paolo Minero, *Member, IEEE*, and Fulvio Schettino, *Member, IEEE*

***Abstract*—The problem of determining the number of spatial degrees of freedom (d.o.f.) of the signals carrying information in a wireless network is reduced to the computation of the geometric variation of the environment with respect to the cut through which the information must flow. Physically, this has an appealing interpretation in terms of the diversity induced on the cut by the possible richness of the scattering environment. Mathematically, this variation is expressed as an integral along the cut, which we call *cut-set integral*, and whose scaling order is evaluated exactly in the case of planar networks embedded in arbitrary three-dimensional (3-D) environments. Presented results shed some new light on the problem of computing the capacity of wireless networks, showing a fundamental limitation imposed by the size of the cut through which the information must flow. In an attempt to remove what may appear as apparent inconsistencies with previous literature, we also discuss how our upper bounds relate to corresponding lower bounds obtained using the techniques of multihop, hierarchical cooperation, and interference alignment.**

***Index Terms*—Capacity, degrees of freedom (d.o.f.), interference, scaling laws, wireless networks.**

I. Introduction

INTERFERENCE is one of the key aspects of a wireless network. Transmitted electromagnetic signals propagate in the environment through line of sight, reflection, diffraction, and scattering. Received signals are given by the superposition of the propagating signals, plus thermal noise. A precise mathematical model of this process is crucial to determine the ultimate limits of communication that can be achieved through cooperation of the network's nodes. This paper attempts a characterization of the interference in terms of signal diversity available at the receivers, which is then related to the amount of information that can be transmitted through wave propagation.

Manuscript received May 01, 2010; revised October 01, 2010; accepted January 19, 2011. Date of current version April 20, 2011. This work was supported in part by the National Science Foundation awards CNS-0916778, CCF-0916465, and CNS 0546235. The material in this paper was presented at the International Conference on Electromagnetics in Advanced Applications (ICEAA 2009) and at the IEEE International Symposium on Information Theory (ISIT 2010).

M. Franceschetti is with the Advanced Network Science Group (ANS), California Institute of Telecommunications and Information Technologies (CALIT2), Department of Electrical and Computer Engineering, University of California, San Diego, CA 92093 USA (e-mail: massimo@ece.ucsd.edu).

M. D. Migliore and F. Schettino are with the Microwave Laboratory at the DAEIMI, University of Cassino, 03043 Cassino (FR), Italy (e-mail: mdmiglio@unicas.it; schettino@unicas.it).

P. Minero is with the Electrical Engineering Department, University of Notre Dame, Notre Dame, IN 46556 USA (e-mail: pminero@nd.edu).

Communicated by S. A. Jafar, Associate Editor for the special issue on "Interference Networks".

Digital Object Identifier 10.1109/TIT.2011.2120150

A wireless interference network is composed of a set of sources $\mathcal{S}$, a set of destinations $\mathcal{D}$, and a set of relays $\mathcal{R}$. Let $\mathcal{T} = \mathcal{S} \cup \mathcal{R}$ and assume that the cardinality of all of these sets is proportional to n. Each node in $\mathcal{S}$ wants to communicate with a corresponding node in $\mathcal{D}$, and all transmissions occur in a given spatial domain and in a narrow frequency band around the same carrier frequency. Interference is modeled as linear superposition of the propagating signals at the receiver. An information-theoretic model of the above scenario is that of a linear transformation of complex random processes, plus additive noise

$$\mathbf{Y}(t) = \mathbf{H}(t)\mathbf{X}(t) + \mathbf{Z}(t), \quad t \in \mathbb{R}_0^+.$$

$\mathbf{X}(t)$ is the random vector process representing the signals transmitted by the sources and the relays, $\mathbf{Y}(t)$ represents the signals received by the destinations, $\mathbf{Z}(t)$ is a vector of complex, circularly symmetric white Gaussian processes of zero mean and unit variance. Transmitted and received signals are modeled as random, complex waveforms, representing amplitude and phases of real transmitted and received sinusoidal signals. The elements of the matrix $\mathbf{H}(t)$ are complex channel coefficients representing the attenuation and phase shifts between transmitters and receivers. These coefficients model the state, at time t, of the physical propagation channel. Given the environment and the positions of the nodes, they are deterministically dictated by the physics of the propagation process. This deterministic point of view is the main *leitmotiv* of this paper. It contrasts with the classic information-theoretic approach that assumes a stochastic space-time model for $\mathbf{H}(t)$.

Considering coding across time blocks of T seconds, all transmitted codewords are subject to the unit power constraint

$$\int_T |X_s(t)|^2 dt \le T \quad \forall s \in \mathcal{T}$$

which implies the total power constraint:[1]

$$\sum_{s\in\mathcal{T}} \int_T |X_s(t)|^2 dt \le nT = O(n), \quad \text{as } n \to \infty. \tag{1}$$

A long standing open problem is determining the optimal strategy of operation of the network modeled above. Several proposals have been made in the literature, which we briefly describe below.

[1]Throughout the paper we use the following subset of the Bachman-Landau notation for positive functions of the natural numbers: $f(n) = O(g(n))$ as $n \to \infty$ if $\exists k > 0, n_0 : \forall n > n_0\ f(n) \le kg(n)$; $f(n) = \Omega(g(n))$ as $n \to \infty$ if $g(n) = O(f(n))$; $f(n) = \Theta(g(n))$ as $n \to \infty$ if $f(n) = O(g(n))$ and $f(n) = \Omega(g(n))$. The intuition is that f is asymptotically bounded up to constant factors from above, below, or both, by g.

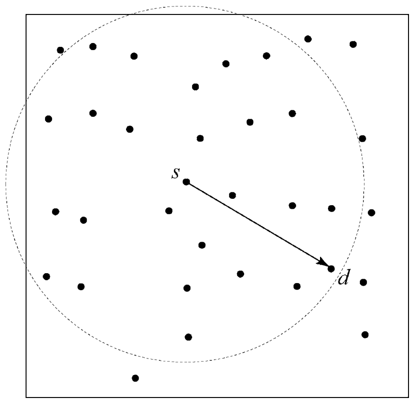

Fig. 1. TDMA-direct scheme. In this strategy there is no spatial reuse of the channel.

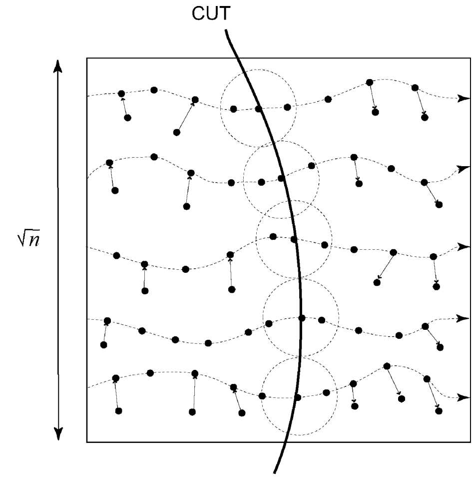

Fig. 2. TDMA-multihop scheme. This strategy is characterized by spatial reuse, but no diversity due to the physical propagation channel is exploited.

A. TDMA-Direct

The simplest strategy of operation is time division multiple access (TDMA) with direct transmission between sources and destinations. In this case, time is divided into slots and in turn each node in $\mathcal{S}$ transmits to its intended destination in $\mathcal{D}$ during its assigned time slot. Relay nodes are not used. Assuming unit bandwidth, the Shannon-Hartley formula yields an information rate per-source destination pair of at most

$$R(n) \leq \frac{1}{n} \log \left(1 + \max_{s \in \mathcal{S}, d \in \mathcal{D}, t \in [0,T]} |H_{sd}(t)|^2\right) = O(1/n)$$

as $n \to \infty$, where the equality holds because the term inside the logarithm depends only on the model chosen for the propagation channel and is independent of n. This situation is depicted in Fig. 1 and we make note that it is characterized by time reuse, but no spatial reuse of the channel.

B. TDMA-Multihop

Time reuse is combined with spatial reuse by adopting a TDMA strategy in conjunction with multihop relay. In this case, routing paths are established between sources and destinations and point-to-point coding and decoding is performed at each hop along the paths, using a TDMA scheme to control the total amount of interference at each transmission, which is treated as noise. Following the first work of Gupta and Kumar [1], this scheme has been analyzed under a variety of models for the propagation channel, see [2]–[5]. In a geometric setting in which nodes are scattered in a region of the plane proportional to n, and sources, destinations, and relays are randomly selected, it leads to a lower bound of

$$R(n) \geq \Omega(1/\sqrt{n}), \quad \text{as } n \to \infty$$

a great improvement compared to the TDMA-direct scheme.

The bound can be intuitively explained as follows. Due to the random assignment of sources, destinations, and relays, roughly half of the nodes located on one side of the network wish to communicate to another half located on the other side. The rate that each source can sustain to its intended destination depends on the number of routing paths that can be established simultaneously across the cut that separates these two regions. We can construct these paths by letting each node select, as the next relay, a nearby neighbor located at most at a constant distance from it. In this way, each hop transmission generates a small interference footprint around it. If routing paths crossing the cut are sufficiently spaced from each other, so that the corresponding interference footprints do not overlap too much, then the total amount of interference at each hop can be controlled using a TDMA scheme and the routes can be performed simultaneously, at constant rate. Since the number of nodes accessing these paths is of the order of n and the number of paths crossing the cut and spaced by at least a constant distance is proportional to the length of the cut, i.e., it is of the order of $\sqrt{n}$, the result then follows. This situation is depicted in Fig. 2, and we make note that it is characterized by spatial reuse, but no diversity due to the physical propagation channel is exploited.

C. MIMO-Hierarchical Cooperation

Hierarchical cooperation is a network strategy originally proposed by Özgür, Lévêque, and Tse [6], although some ideas were also present in the work of Aeron and Saligrama [7]. The objective of the strategy is to exploit the spatial diversity provided by the physical propagation channel to achieve a better capacity scaling. The network area is recursively divided into clusters and within each cluster nodes form a distributed single-user multiple antenna system (MIMO) performing joint encoding and communicating with the nodes in another cluster that perform joint decoding. Within each cluster, information is then redistributed recursively by iterating the above scheme. This situation is depicted in Fig. 3. Under certain stochastic assumptions on the matrix $\mathbf{H}(t)$, and knowledge of its realization at all nodes, each MIMO transmission can achieve a rate that is proportional to the number of transmitting antennas, and this allows the per-node rate to remain almost constant, as the total number of nodes, and the number of recursive layers, grows. A great improvement compared to the multihop case. Precise scaling laws have been worked out in [8] and [9].

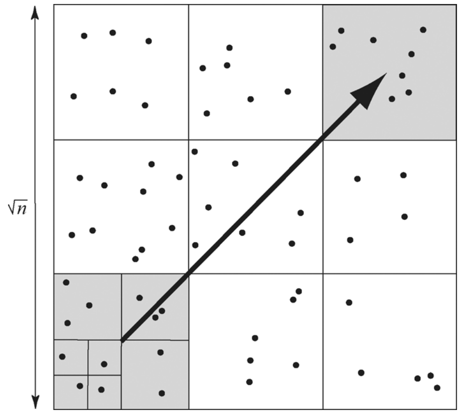

Fig. 3. Hierarchical cooperation. The spatial diversity provided by the propagation channel is exploited at each MIMO transmission.

The strategy requires to assume a specific stochastic model of the physical propagation channel to obtain the promised advantage over the multihop scheme. Accordingly, $\mathbf{H}(t)$ is modeled as a random matrix, whose elements are

$$H_{kl}(t) = r_{kl}^{-\alpha} e^{ju_{kl}(t)} \quad (2)$$

where r_{kl} is the (random) distance between the kth transmitter and the lth receiver and $1 < \alpha < 2$ is a constant. The phase shifts $u_{kl}(t)$ are white random processes, uniform in $[0, 2\pi]$ and independent in k, l. Hence, the magnitude of the channel coefficients tends to zero as a small power of the distance (path loss assumption), and the phases vary randomly with time and space in a uniform independent and identically distributed (i.i.d.) fashion (fading assumption). We make note that this strategy exploits the diversity due to the physical propagation channel through repeated MIMO transmissions.

D. Interference Alignment

Interference alignment is another strategy that exploits the diversity due to the physical propagation channel. It was proposed by Cadambe and Jafar [10] and Maddah-Ali, Motahari, and Khandani [11]. The main idea is that assuming $\mathbf{H}(t)$ varies randomly, one can perform coding over many realizations, and transmit codewords that span a subspace where they overlap, at all the receivers where they constitute interference, and a subspace where they remain decodable, at the intended destinations. Recently, Özgür and Tse [12] have shown that interference alignment can achieve the same performance as hierarchical cooperation, under the same stochastic model of the propagation channel given in (2). We make note that these results also rely on the diversity introduced by the stochastic model of the propagation channel.

E. Our Contribution

All the constructive strategies described above must obey the information-theoretic cut-set upper bound [13]. An easy statement of this in our context is as follows. Letting n nodes be distributed arbitrarily on either side of a cut which divides the network into two parts, we have

$$R(n) \leq \frac{1}{n} \max_{t \in [0,T]} \text{ rank } \mathbf{H}(t) O(\log n), \quad \text{as } n \to \infty. \quad (3)$$

In words, one can at most beamform the total power into each of the equivalent point to point channels provided by the matrix $\mathbf{H}(t)$.

This paper studies $\max_{t \in [0,T]} \text{rank}\mathbf{H}(t)$ from first physical principles, and shows that a natural upper bound, over all scattering environments and node locations, exists and depends on the geometric variation of the environment with respect to the cut through which the information must flow. We call this maximum value the *number of degrees of freedom (d.o.f.)* of the wireless network. Mathematically, it can be upper bounded by an integral, that we call *cut-set integral*. This bound can then be used to determine in what environments the stochastic assumptions of the strategies described above could be valid, and in what environments these assumptions fail. Hence, our focus is not to design novel achievable coding schemes, but rather to derive information-theoretic outer bounds on what physics permits to achieve.

The rest of the paper is organized as follows. The next section provides a summary of the results and of the technical approach used in the analysis. Section III relates the physics of the propagation process to the information-theoretic model, and formally introduces the number of d.o.f. of the radiated field. The following two sections are devoted to computing upper bounds on the number of d.o.f. by using two different methods: in Section IV we follow a singular value decomposition approach; in Section V we follow a spatial bandwidth approach, introduce the concept of cut-set integral, and then provide solutions to this integral in two geometric settings of practical interest. Section VI draws conclusions and provides some final observations.

II. Statement of Results

A. Geometric Configurations

In a previous work, the number of d.o.f. of wireless networks in two-dimensional (2-D) and three-dimensional (3-D) settings has been studied from first physical principles [14]. Considering a scale-free model in which all distance lengths are normalized by the carrier wavelength, it has been shown that when nodes are distributed inside a disc of area proportional to n in such a way that roughly n sources lie inside the inner half of the disc and wish to communicate with n destinations in the outer annulus, then the number of d.o.f. is bounded by an order of $n^{1/2} \log n$. This bound holds for any scattering environment and node locations inside the disc. Similarly, when an order of n nodes are distributed inside a ball of volume proportional to n, then the number of d.o.f. is bounded by an order of $n^{2/3} (\log n)^2$. These configurations are depicted in Fig. 4(a) and (b).

In this paper, we consider the two configurations of planar networks depicted in Fig. 4(c) and (d), as well as develop a general method to bound the number of d.o.f. in arbitrary geome-

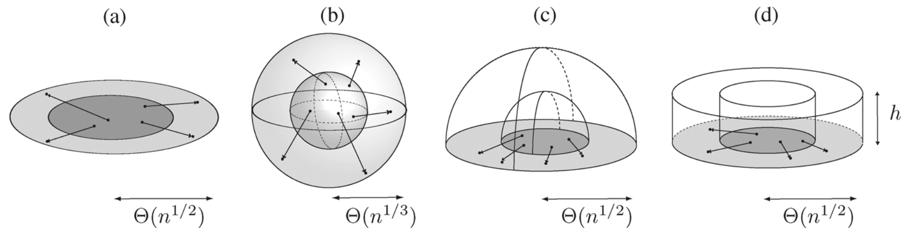

Fig. 4. Some canonical geometries.

tries having rotational symmetry. As before, all distance lengths are normalized to the wavelength, so that the configurations are scale-invariant. The considered geometries have the advantage of decoupling the effect of the environment from the network. In the first case, an order of n nodes are placed on the base of a half sphere of area proportional to n and are surrounded by an arbitrary scattering environment of volume proportional to $n^{3/2}$. In the second case, an order of n nodes are placed on the base of a cylinder of area proportional to n and are surrounded by an arbitrary scattering environment of volume proportional to $h \times n$, where h is a given constant. We show that the number of d.o.f. in the first case can be as large as n, while in the second case it is bounded by an order of $h\sqrt{n}(\log n)^2$.

These results suggest that while a scattering environment that is large compared to the number of nodes inside it (half sphere case) does not provide a bottleneck to the number of d.o.f., the environment becomes a bottleneck when its size is comparable to the number of nodes inside it (disc, sphere, cylinder cases).

Finally, a precise quantification of the available spatial resource is given in the more general setting of arbitrary geometries having rotational symmetry, introducing the notion of cut-set integral, a geometric measure of the richness of the scattering environment induced on the network cut through which the information must flow.

B. Technical Approach

Our approach is based on the functional analysis of the vector space spanned by the electromagnetic field propagating in the environment. After drawing a correspondence between the information-theoretic channel and the electromagnetic vector space, we evaluate the dimensionality of this space using two different methods. The first one determines the number of significant singular values that are sufficient to construct a finite-rank approximation of the propagation operator. This is the same method as the one used in [14], applied to different geometric configurations. It has the appeal of revealing the natural phase transition of the number of independent channels available in the environment. However, for one of the two considered geometries, it requires some additional assumptions to obtain closed form solutions. The second method computes the number of d.o.f. as a cut-set integral using reconstruction by space-bandlimited functions. This allows an exact analytical representation of the scaling order of the number of d.o.f., for the two geometries of interest. It can in principle be applied to any geometry having rotational symmetry and it leads to the natural interpretation of the cut-set integral as the amount of diversity induced on the cut by the possible richness of the scattering environment. The roots of both strategies are in the papers of Bucci and Franceschetti [16], [17], subsequently expanded by Bucci, Gennarelli, and Savarese [18]. We outline the main steps of their methods required in our case, extend the theory to general two-dimensional cut-sets, and finally provide an application to the two specific network geometries of interest.

III. Setting Up the Problem

A. Information-Theoretic and Physical Channel Model

With reference to the half-sphere and cylinder depicted in Fig. 4(c) and (d), we consider communication from n nodes placed inside the inner disc on the base of the half-sphere, or cylinder, to n nodes placed in the outer annulus. We call the corresponding inner and outer volumes separated by the surface cut which divides the half-sphere or cylinder in half, D and V, respectively. We introduce an arbitrarily small constant separation distance δ between these two volumes. This ensures that transmitters and receivers do not coincide so that the kernel of the propagation operator does not have singularities. We consider empty space outside D, as the presence of scatterers in V does not increase the number of d.o.f. The heuristic justification is that a closed surface captures the whole information flow radiating out of D and so backscattering does not increase the number of d.o.f. A more rigorous argument appears in [14, Sec. III-B].

The information-theoretic representation of the channel is depicted in Fig. 5(a). The narrowband signal $\mathbf{X}(t)$ is a sinusoidal waveform modulated by some input symbols. The effect of the physical propagation process is modeled as of producing a phase-shifted and magnitude-attenuated copy of the transmitted waveform. The spatial variation of the environment and node positions over time is captured by a random variation of the attenuation and phase shift over time. A commonly used model is to assume the attenuation being fixed and the phase shift to evolve randomly over time in an i.i.d. fashion, see (2). This corresponds to having small scale movements in the environment of the order of the wavelength, which affect only the phase but not the magnitude of the received waveform. This variation due to environmental effects does not change the narrowband nature of the signal.

The corresponding physical picture is depicted in Fig. 5(b). An operator $\mathcal{F}$ maps the input signal $\mathbf{X}(t)$ into a certain current density inside the inner volume D. This includes both the source currents on the transmitting antennas and the induced currents on the antennas and the scatterers. Its space-time representation

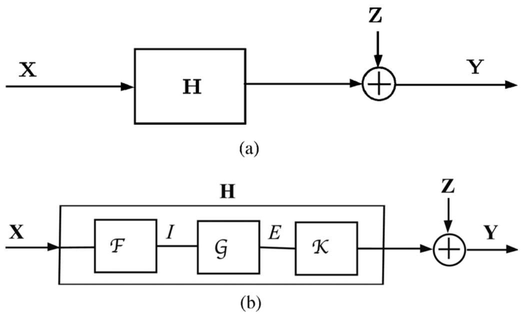

Fig. 5. Block diagram of the communication operator. (a) Information-theoretic model. (b) Physical model.

is given by $i(\mathbf{r}_d, t)$. The total power constraint in (1) translates into the equivalent constraint

$$\int_T dt \int_D |i(\mathbf{r}_d, t)|^2 d\mathbf{r}_d \leq nT = O(n), \quad \text{as } n \to \infty. \tag{4}$$

The current density may change over time due to the modulation of the signal by the input symbols and to variations in the environment and node positions. At any time, we assume an *arbitrary* distribution, as long as it occupies a narrow frequency band and it satisfies (4). Hence, the fading process that is modeled by a stochastic variation of $\mathbf{H}(t)$ in the information-theoretic model, is accounted here by considering, at any time, an arbitrary current density inside D satisfying the total power constraint (4).

We write the space-frequency representation of the current, obtained by taking the temporal Fourier transform, as $I(\mathbf{r}_d, f)$. By the narrowband nature of the signals, we can suppress the dependence on frequency from the notation above and write $I(\mathbf{r}_d)$. We proceed performing an harmonic analysis around frequency f.

Let us define the Hilbert space $\mathcal{I} \subseteq L_2(D)$ of square integrable functions of support D with inner product

$$\langle I, I' \rangle_{\mathcal{I}} \equiv \int_D I^*(\mathbf{r}_d) I'(\mathbf{r}_d) d\mathbf{r}_d$$

where $*$ denotes the complex conjugate. By Parseval theorem, the power constraint (4) can then be rewritten as

$$||I||^2_{\mathcal{I}} \equiv \langle I, I \rangle_{\mathcal{I}} = O(n), \quad \text{as } n \to \infty.$$

The current density generates a narrowband electric field $E(\mathbf{r})$ which is measured in a domain V strictly outside the volume D. The measured field belongs to the Hilbert space $\mathcal{E} \subseteq L_2(V)$ with inner product given by

$$\langle E, E' \rangle_{\mathcal{E}} \equiv \int_V E^*(\mathbf{r}) E'(\mathbf{r}) d\mathbf{r}.$$

The operator $\mathcal{G} : \mathcal{I} \to \mathcal{E}$ that maps the current into the field is given by

$$E(\mathbf{r}) = (\mathcal{G}\, I) = \int_D \mathcal{G}(\mathbf{r}_d, \mathbf{r}) I(\mathbf{r}_d) d\mathbf{r}_d, \quad \mathbf{r} \in V. \tag{5}$$

Having normalized all distances by the wavelength, in free space, we have

$$\mathcal{G}(\mathbf{r}_d, \mathbf{r}) = -\frac{j\sqrt{\mu_0}}{2\sqrt{\epsilon_0}} \left(\bar{I} + \frac{\nabla\nabla}{(2\pi)^2} \right) \frac{e^{-j2\pi|\mathbf{r}_d - \mathbf{r}|}}{|\mathbf{r}_d - \mathbf{r}|}$$

where $\bar{I}$ is the identity operator, μ_0 and ϵ_0 are the permeability and permittivity of the vacuum. Since the domains D and V are disjoint, the kernel in (5) is square integrable and the radiation operator $\mathcal{G}$ is compact.

Finally, an operator $\mathcal{K}$ maps the field to the voltage measured at the receiving antennas, and the additive noise is the same in the two models.

B. The Degrees of Freedom of the Radiated Field

Let $\mathcal{E}_N \subseteq \mathcal{E}$ be an N-dimensional subspace of $\mathcal{E}$. The *deviation* of $\mathcal{E}_N$ from $\mathcal{E}$ is defined as

$$\Delta(\mathcal{E}, \mathcal{E}_N) = \sup_{E \in \mathcal{E}} \inf_{E' \in \mathcal{E}_N} ||E - E'||_{\mathcal{E}}.$$

The Kolmogorov N-*width*, or N-diameter, of $\mathcal{E}$ is defined as

$$d_N(\mathcal{E}) = \inf_{\mathcal{E}_N} \Delta(\mathcal{E}, \mathcal{E}_N) \tag{6}$$

where the infimum is taken over all subspaces of $\mathcal{E}$ of finite dimension N [22, Ch. I]. The quantity (6) characterizes the best accuracy obtained by approximating the space of radiated fields $\mathcal{E}$ by an N-dimensional subspace of $\mathcal{E}$. Given a level of accuracy $\epsilon > 0$, the *number of d.o.f.* of the radiated field is defined as

$$N_\epsilon(\mathcal{E}) = \min\{N : d_N(\mathcal{E}) \leq \epsilon\}.$$

Thus, $N_\epsilon(\mathcal{E})$ denotes the dimension of the minimal subspace representing the radiated field in V within an ϵ accuracy.

Remark: Since we deal with continuous fields, the definition of d.o.f. naturally depends on the accuracy level ϵ of the approximation and it is different from the usual information-theoretic definition. For a discussion of the significance of this approach we refer to the classic work of Slepian [19] which adopts the same point of view of *natura non facit saltus* as the one of this paper. It turns out that due to a sharp threshold transition behavior of $d_N(\mathcal{E})$, the number of d.o.f. as defined above is weakly dependent on ϵ, which makes the definition quite suitable for practical scenarios. In Slepian's own words: *in relevant mathematical models of the real world, principal quantities of the model such as the number of d.o.f.] must be insensitive to small changes of secondary quantities of the model [such as the precision ϵ of the measurement apparatus].*

The d.o.f. as defined above were introduced in [17]. They can also be interpreted in terms of the Kolmogorov ϵ-entropy, see [17], [20]. The correspondence with the number of spatial modes that are physically separable and available for communication was also given in [21]. This correspondence was also used in [14] to evaluate the cut-set bound (3) for the geometries depicted in Fig. 4(a) and (b). Next, we consider the geometries in Fig. 4(c) and (d).

IV. The Singular Value Decomposition Approach

The N-diameter of $\mathcal{E}$ and the number of d.o.f. can be evaluated via the singular value decomposition of the radiation operator $\mathcal{G}$ [22, Ch. IV]. Let $\mathcal{G}^\dagger : \mathcal{E} \to \mathcal{I}$ denote the adjoint operator of $\mathcal{G}$, defined by $\langle \mathcal{G}\, I, E\rangle_{\mathcal{E}} = \langle I, \mathcal{G}^\dagger E\rangle_{\mathcal{I}}$. The singular value decomposition of $\mathcal{G}$ can be obtained from the eigendecomposition of the associated self-adjoint compact operators $\mathcal{G}^\dagger\mathcal{G} : \mathcal{I} \to \mathcal{I}$ and $\mathcal{G}\mathcal{G}^\dagger : \mathcal{E} \to \mathcal{E}$, considering the following eigenvalue problems:

$$\begin{cases} (\mathcal{G}^\dagger\mathcal{G}\; v_k)(\mathbf{r}) = \sigma_k^2 v_k(\mathbf{r}) \\ (\mathcal{G}\mathcal{G}^\dagger\; u_k)(\mathbf{r}) = \sigma_k^2 u_k(\mathbf{r}) \end{cases}, \quad k = 1, 2, \dots \tag{7}$$

The eigenvectors $\{v_k\}$ and $\{u_k\}$ are the right and left singular functions of the operator $\mathcal{G}$, respectively, while the coefficients σ_k are the singular values of $\mathcal{G}$. The compactness of $\mathcal{G}$ implies that the eigenvectors $\{v_k\}$ and $\{u_k\}$ form a complete orthogonal basis set for $\mathcal{I}$ and $\mathcal{E}$, respectively, and the singular values are nonnegative real numbers. Expanding the integral kernel in (5) in terms of the singular functions, we obtain the following singular value decomposition of $\mathcal{G}$:

$$E(\mathbf{r}) = (\mathcal{G}\; I)(\mathbf{r}) = \sum_{k=1}^{\infty} \sigma_k \langle I, v_k\rangle_{\mathcal{I}}\; u_k(\mathbf{r}), \quad \mathbf{r} \in V. \tag{8}$$

This shows that the field due to the current $I \in \mathcal{I}$ is the linear combination of the left singular functions $\{u_k\}$, and that the weight given to the kth term in the summation is the product of the kth singular value and the projection of I onto the right singular function v_k.

The following theorem provides the connection between the number of d.o.f. of the radiated field and the singular value decomposition of $\mathcal{G}$.

Theorem 4.1: [22, Theorem 2.5, p. 69] Let the singular values $\{\sigma_k\}$ in (7) be ordered in decreasing order of magnitude $\sigma_1 \geq \sigma_2 \geq \cdots \geq \sigma_k \geq \sigma_{k+1} > 0$, $k > 2$. Then,

$$d_N(\mathcal{E}) = \sigma_{N+1}, \quad N = 1, 2, \dots$$

and an optimal N-dimensional subspace $\mathcal{E}_N$ for which $\Delta_N(\mathcal{E}, \mathcal{E}_N) = d_N(\mathcal{E})$ is given by $\mathcal{E}_N = \mathrm{span}\{u_1, \dots, u_N\}$.

It follows that the N-widths of the radiation operator $\mathcal{G}$ are determined precisely by the behavior of the $(N+1)$th singular value σ_{N+1}, and that to achieve the optimal representation of the field it suffices to approximate the image of any $I \in \mathcal{I}$ under $\mathcal{G}$ by the first $N+1$ terms of the singular value decomposition (8). Since for compact operators $\lim_{k\to\infty} \sigma_k = 0$, it is possible to approximate the radiated field at any desired level of accuracy ϵ by choosing N large enough, and the d.o.f. are determined by the index of the first singular value having magnitude smaller than ϵ.

A. Application to the Half-Sphere

The treatment is similar to the one for spherical geometries in [14], Section IV. Hence, only the relevant steps are summarized in what follows. Consider the configuration depicted in Fig. 4(c). The domain D, containing the source nodes on its base, is the half-sphere of radius $\sqrt{n}$ centered at the origin; the domain V, containing the destination nodes, is the outer spherical half-annulus obtained subtracting D from a half-sphere of radius $2\sqrt{n}$ centered at the origin. Let M denote the surface of the sphere of radius $\sqrt{n} + \delta$ centered at the origin. Since M encloses the domain of the sources, the field on M uniquely determines the field at any point in V. Thus, it suffices to determine the number of d.o.f. of the field on M.

Following [14], we refer to the magnetic vector potential $A \in \mathcal{A} \subseteq L_2(M)$, and perform the singular value decomposition of the Green function G that maps the source current density I to the magnetic vector potential. Analogous results can be obtained using the multipole expansion of the electric field [23] for spherical sources, and performing the singular value decomposition of the of the dyadic Green function $\mathcal{G} : \mathcal{I} \to \mathcal{E}$, instead than of $G : \mathcal{I} \to \mathcal{A}$.

The Green function operator for the magnetic vector potential is given by

$$A(\mathbf{r}) = (GI) = \int_D G(\mathbf{r}_d, \mathbf{r}) I(\mathbf{r}_d) d\mathbf{r}_d, \quad \mathbf{r} \in M \tag{9}$$

where

$$G(\mathbf{r}_d, \mathbf{r}) = \frac{e^{-j2\pi|\mathbf{r}_d - \mathbf{r}|}}{4\pi|\mathbf{r}_d - \mathbf{r}|}.$$

The singular value decomposition of the operator in (9) was evaluated in [14], Section IV. Given this decomposition, we have the following result, proven in the Appendix.

Theorem 4.2: For any $\epsilon > 0$

$$N_\epsilon(\mathcal{A}) = \Omega(n), \quad \text{as } n \to \infty.$$

The above shows that the number of d.o.f. of the magnetic vector potential scales *at least* linearly in n, as $n \to \infty$. The electromagnetic field is obtained from the magnetic vector potential through differentiation operations which do not decrease the number of d.o.f. It follows that it is not possible to approximate the field within any constant error by interpolating less than an order of n functions.

The considered geometrical configuration provides an example of a wireless network for which the number of d.o.f. provided by the large scattering environment that surrounds the nodes in space is not a limitation to communication, as it scales proportionally to the *surface* of the sphere enclosing sources and scattering objects. The size of the spatial cut separating the sources from the destinations can be interpreted here as a resource to be shared by the independent communication channels, each of which occupies a fraction of space on this cut.

B. Application to the Cylinder

Consider now the cylindrical geometry illustrated in Fig. 4(d), in which n nodes are placed inside a disc of radius $\sqrt{n}$ and wish to communicate to n nodes which lie inside the annulus formed subtracting the domain of the sources from a concentric disc of radius $\sqrt{n}$, and where scattering objects can be arbitrarily placed inside the cylindrical volume of height h.

The singular value decomposition of the operator (9) in this geometric setup does not seem to be analytically tractable. We outlined an approximate computation in [15], which we do not wish to repeat here, by assuming the two discs at the bases of the cylindrical domain to be infinite planar electric conductors. With this approximation, the singular values exhibit a step-like behavior around the value $h\sqrt{n}$.

This suggests that the number of d.o.f. of the radiation operator scales proportionally to the lateral *surface* of the cylinder enclosing the sources. We make note that the lateral surface of the cylinder represents the cut through which the information must flow and can be interpreted as the spatial resource to be shared by the independent communication channels, each of which occupies a fraction of space on this cut. In the next section, we rigorously prove the above statements using a different method which does not require any approximation. Furthermore, this method can be applied to any geometric setting with rotational symmetry.

V. Cut-Set Integral Approach

In this section, we consider a general geometric setting where the radiating sources are enclosed in a convex domain with rotational symmetry, and the field is observed over a two-dimensional domain having rotational symmetry.

Extending the theory developed by Bucci and Franceschetti [16], [17], and by Bucci, Gennarelli, and Savarese [18], we approximate the radiated field using *spatial bandlimited functions*. The number of d.o.f. of the radiated field is then upper bounded by the Nyquist number associated to this approximation. The bandwidth is determined by choosing an appropriate parametrization of the surface representing the cut through which the information must flow, and it is given in terms of an integral that we call *cut-set* integral.

After outlining the general theory, we apply it to evaluate an upper bound to the number of d.o.f. for the half-sphere and cylinder geometries illustrated in Fig. 4(c) and (d).

A. One-Dimensional Cut-Set

We briefly review the results in [16]–[18] necessary for our derivation. All lengths are normalized by the wavelength. We consider the field radiated by finite size sources enclosed in a convex domain D and observed over a one-dimensional analytic curve M of length S. Let the maximal radial component of both D and M be $\Theta(\sqrt{n})$. Let $\xi : M \to \mathbb{R}$ denote a parametrization of the observation curve. Let $s : M \to [0, S]$ denote the arc-length coordinate along the observation curve M and let $\hat{\mathbf{t}}$ denote the unit vector tangent to s.

Given a point $\mathbf{r}(s) \in M$ and a point $\mathbf{r}_d \in D$, let $\mathbf{R} = \mathbf{r}(s) - \mathbf{r}_d$, and let $\hat{\mathbf{R}}$ be the unit vector of $\mathbf{R}$, see Fig. 6. Define now the *reduced field*

$$F(\xi) = E(\xi)e^{j\psi(\xi)} \tag{10}$$

where ξ is the arbitrary parametrization of the observation curve M, and ψ is an arbitrary analytical phase factor. The extraction of an appropriate phase factor along the curve will lead to a spatial baseband representation of the field. We make note that

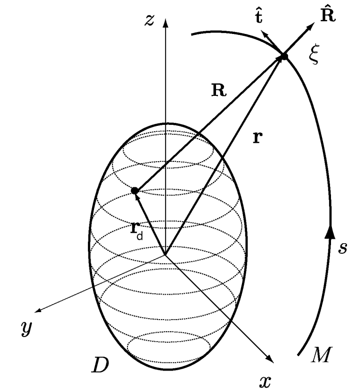

Fig. 6. The case of a one-dimensional observation domain.

this operation does not change the information content of the field. Substituting (5) into (10), we have

$$F(\xi) = (\mathcal{G}'I) = \int_D \mathcal{G}(\mathbf{r}_d, \xi)e^{j\psi(\xi)}I(\mathbf{r}_d)d\mathbf{r}_d$$

where $\mathcal{G}'$ denotes the operator that maps the current I to the reduced field.

Our objective is to approximate $F(\xi)$ using fields with bandwidth w, and to do so we consider the bandlimited reduced field obtained by convolving F with a sinc function in the ξ domain[2]

$$F_w(\xi) = \frac{1}{\pi}\frac{\sin w\xi}{\xi} * F(\xi),$$

where $*$ denotes the convolution operator. We can now define a dyadic Green function $\mathcal{G}'_w(\mathbf{r}_d, \xi(\mathbf{r}))$ for the bandlimited reduced field $F_w(\xi)$ as follows:

$$\begin{aligned} F_w(\xi) &= (\mathcal{G}'_w I) \\ &= \frac{1}{\pi}\int_D \int_{-\infty}^{\infty} \frac{\sin w(\xi - \xi')}{\xi - \xi'}\mathcal{G}'(\mathbf{r}_d, \xi')d\xi' I(\mathbf{r}_d)d\mathbf{r}_d. \end{aligned}$$

The representation error in approximating F by F_w is given by

$$\Delta F(\xi) = F_w(\xi) - F(\xi) = \int_D \Delta\mathcal{G}(\mathbf{r}_d, \xi)I(\mathbf{r}_d)d\mathbf{r}_d.$$

where $\Delta\mathcal{G}(\mathbf{r}_d, \xi) = \mathcal{G}'_w(\mathbf{r}_d, \xi) - \mathcal{G}'(\mathbf{r}_d, \xi)$, so that we have, for all ξ,

$$\| \Delta F(\xi) \|^2_{\mathcal{E}} \leq \max_{\mathbf{r}_d} |\Delta\mathcal{G}(\mathbf{r}_d, \xi)|^2 \| I \|^2_{\mathcal{I}} .$$

Notice that the above is obtained by maximizing over $\mathbf{r}_d$, i.e., considering all possible scatterers' configurations inside D.

The asymptotic behavior of $|\Delta\mathcal{G}(\mathbf{r}_d, \xi)|$ as $n \to \infty$ is studied by the steepest descent method in [17]. The main idea of this method is to reduce the computation of the complex integrals appearing in $|\Delta\mathcal{G}(\mathbf{r}_d, \xi)|$ to asymptotically equivalent ones that can be explicitly evaluated.

[2]Equivalently, for closed curves the convolution is with the Dirichlet kernel $D_w(\xi)$ which gives the wth degree Fourier series approximation to the periodic F.

It turns out that letting

$$w(\xi) = \max_{\mathbf{r}_d} \left| \frac{\partial}{\partial \xi}(\psi(\xi) - 2\pi R(\mathbf{r}_d, \xi)) \right| \tag{11}$$

which is referred to as the *local bandwidth* at point ξ, the error in approximating the reduced field decreases to zero exponentially as the bandwidth w exceeds the critical value $w(\xi)$. Thus, although F is *not* bandlimited in the transformed domain of the parametric coordinate ξ, it can be approximated at any desired level of accuracy via bandlimited functions, provided that the bandwidth is sufficiently larger than $w(\xi)$. More precisely, given any desired level of accuracy $\epsilon > 0$ there exists an $\chi > 1$ such that

$$|\Delta F(\xi)| \leq \epsilon, \quad \text{if } w > \chi w(\xi).$$

Furthermore, as the dimension of the system increases, i.e., as $n \to \infty$, we have that $\chi = 1 + O(n^{-2/3}) \to 1$, so that the reduced field tends to become bandlimited.

The phase factor ψ can now be chosen such that the critical value $w(\xi)$ is minimized for all ξ. This can be accomplished by letting

$$\frac{d\psi}{d\xi} = \pi \left(\max_{\mathbf{r}_d} \frac{\partial R}{\partial \xi} + \min_{\mathbf{r}_d} \frac{\partial R}{\partial \xi} \right)$$

which can be plugged back into (11) obtaining

$$w(\xi) = \pi \left(\max_{\mathbf{r}_d} \frac{\partial R}{\partial \xi} - \min_{\mathbf{r}_d} \frac{\partial R}{\partial \xi} \right). \tag{12}$$

Next, we choose the parametrization ξ of the observation domain so that w is constant along the curve, i.e., $w(\xi) = W$ for all $\xi \in M$. For this parametrization, the field at any point on the curve M is now arbitrarily close to one of bandwidth slightly greater than the constant W, and we evaluate its number of d.o.f. in terms of the Nyquist number associated to W. We do so by first substituting into (12)

$$\frac{\partial R}{\partial \xi} = \frac{\partial R}{\partial s} \frac{\partial s}{\partial \xi}$$

obtaining

$$W d\xi = \pi \left(\max_{\mathbf{r}_d} \frac{\partial R}{\partial s} - \min_{\mathbf{r}_d} \frac{\partial R}{\partial s} \right) ds. \tag{13}$$

Then, we integrate along the curve M, obtaining

$$\begin{aligned} W \int_M d\xi &= \pi \int_0^S \left(\max_{\mathbf{r}_d} \frac{\partial R}{\partial s} - \min_{\mathbf{r}_d} \frac{\partial R}{\partial s} \right) ds \\ &= \pi \int_0^S \left(\max_{\mathbf{r}_d} \hat{\mathbf{R}} \cdot \hat{\mathbf{t}} - \min_{\mathbf{r}_d} \hat{\mathbf{R}} \cdot \hat{\mathbf{t}} \right) ds. \end{aligned}$$

Finally, we compute the Nyquist number associated to the bandwidth W as

$$\begin{aligned} N_0 &= \frac{W \int_M d\xi}{\pi} \\ &= \int_0^S \left(\max_{\mathbf{r}_d} \hat{\mathbf{R}} \cdot \hat{\mathbf{t}} - \min_{\mathbf{r}_d} \hat{\mathbf{R}} \cdot \hat{\mathbf{t}} \right) ds. \end{aligned} \tag{14}$$

This dimensionless quantity is the analogous, in the spatial domain, of the communication-theoretic time-bandwidth product. It represents the dimension of the space of signals of bandwidth W, observed over the domain M. Strictly speaking, however, its significance can only be taken in an asymptotic sense, since the only signal that is both bandlimited and spacelimited is the trivial always-zero signal [24]. In practice, the field is only *approximately* bandlimited and it is observed over a *finite* domain. As the system size tends to infinity, the bandlimitation error becomes arbitrarily small, and an accurate field reconstruction is possible interpolating only slightly more than N_0 optimal functions over a finite domain. The basis functions used for the reconstruction are complex exponential functions of ξ, if M is a closed curve, or prolate spheroidal functions, in the case of open observation domains. Formally, in [17] it is established, using results in [22] and [24], that

Theorem 5.1: For any $\epsilon > 0$

$$N_\epsilon(\mathcal{E}) = O\left(N_0 \log \frac{1}{\epsilon}\right), \quad \text{as } n \to \infty$$

so the number of d.o.f. is slightly larger than N_0 and it is practically independent of the error ϵ, in the sense that the error can be $\epsilon_n = O(\frac{1}{N_0^\gamma})$ for any $\gamma > 0$, as $n \to \infty$, and change the scaling order of the number of d.o.f. by at most a logarithmic factor.[3]

Remark: We call (14) the cut-set integral associated to the cut M and the set D. It measures the total incremental variation of the tangential component of $\mathbf{R}$ along the cut M. The physical interpretation is that of measuring the richness of the information content of the field radiated from D, by considering a variational measure of the environment in D with respect to the cut M through which the information must flow. It follows that if the combined effect of the source and the receiver's geometries are such that $\mathbf{R}$ is "highly variable" in the sense of the integral above, then the scattered field has a large information content. We also make note that this notion of boundary measure in the sense of total geometric variation seems related to the more general concept of Caccioppoli sets in mathematics [25].

B. Two-Dimensional Cut-Set

We now generalize the results outlined in the previous section to surface-cuts with rotational symmetry. Given a cylindrical coordinate system (ρ, ϕ, z), consider the field radiated by finite size sources enclosed in a convex domain D bounded by a surface with rotational symmetry, obtained by rotating a curve D' lying in the plane $\phi = 0$ about the z axis. The field is observed over a surface of revolution M external to D and generated by the rotation of a meridian curve M', lying in the plane $\phi = 0$, about the z axis. Let the maximum radial component of both D' and M' be of order $\Theta(\sqrt{n})$.

[3]The result of [17] is actually sharper than what reported here, being $N_\epsilon(\mathcal{E}) = N_0 + O((N_0)^{1/3}(\log 1/\epsilon)^{2/3}) + O(\log N_0 \log(1/\epsilon))$. Our slightly weaker but more compact form is good enough for our purposes and it is chosen to simplify the rest of the presentation.

The electromagnetic field on M can be expanded in a complete orthogonal set of cylindrical vector waves [26]. This representation is given by

$$E(\rho,\phi,z)=\sum_{m=-\infty}^{+\infty}E_m(\rho,z)e^{jm\phi} \tag{15}$$

where each function $E_m(\rho,z)$ corresponds to the two-dimensional electric field generated by the current density $I_m(\rho,z)$, which is the mth term of the Fourier series expansion in the angular domain ϕ

$$I(\rho,\phi,z)=\sum_{m=-\infty}^{+\infty}I_m(\rho,z)e^{jm\phi}.$$

An upper bound on the number of d.o.f. $N_\epsilon(\mathcal{E})$ of the field on M can now be computed proceeding in three steps. First, we consider the electric field measured on the one-dimensional curve M_ϕ obtained by intersecting M with a plane at constant z. We bound the number of d.o.f. of the radiated field measured on the circumference M_ϕ by evaluating the Nyquist number N_0 in (14). Notice that the integrand in (14) is equal to the difference between two cosines and thus it is upper bounded by 2, so N_0 in this case can be bounded by the length of the circumference M_ϕ which is of order $O(\sqrt{n})$. Due to the cylindrical geometry, the extreme values of $\partial R/\partial s$ are opposite and constant along M_ϕ. It follows from (13) that any parametrization ξ proportional to the arc-length is optimal. In particular, we can choose ξ equal to the azimuthal angle ϕ, so the approximating functions used for the reconstruction are the harmonics $\{e^{jm\phi}\}$.

We let $N_0=O(\sqrt{n})$ and, making use of the field representation in (15), define the optimal approximation

$$\hat{E}_{N_0}(\rho,\phi,z)=\sum_{m=-N_0\log(1/\epsilon)}^{+N_0\log(1/\epsilon)}E_m(\rho,z)e^{jm\phi}. \tag{16}$$

In the second step, we approximate each two-dimensional electric field component $E_m(\rho,z)$ in (16) using a suitable minimal set of basis functions. Observe that $E_m(\rho,z)$ does not depend on ϕ, so we can study its characterization on the one-dimensional meridian curve M' lying on the plane $\phi=0$. In order to find a uniform upper bound independent of m, we can assume to have an arbitrary current distribution $I(\rho,z)$ in the domain D' and apply the method illustrated in the previous section to bound the number of d.o.f. of the radiated field $E_m(\rho,z)$ measured on M' by evaluating the corresponding Nyquist number in (14), which we denote by N_0'.

Finally, in the third step, we can combine results and conclude that the overall Nyquist number $N_0^{\rm tot}$ is given by

$$\begin{aligned}N_0^{\rm tot}&=\sum_{m=-N_0}^{N_0}N_0'\\&=O(N_0N_0')\\&=O(\sqrt{n}N_0'),\quad \text{as } n\to\infty.\end{aligned} \tag{17}$$

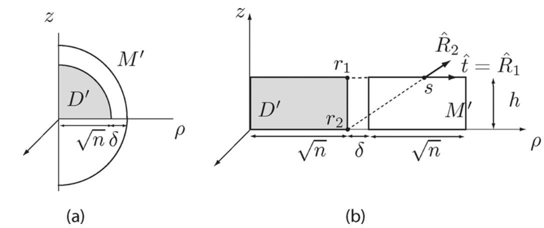

Fig. 7. Construction of the half-sphere and cylinder geometries by rotations.

By Theorem 5.1, we have

$$\begin{aligned}N_\epsilon(\mathcal{E})&=\sum_{-N_0\log(1/\epsilon)}^{N_0\log(1/\epsilon)}N_0'\log(1/\epsilon)\\&=O\left(N_0^{\rm tot}\left(\log 1/\epsilon\right)^2\right)\\&=O(\sqrt{n}N_0'(\log 1/\epsilon)^2),\quad \text{as } n\to\infty.\end{aligned} \tag{18}$$

C. Application to the Half-Sphere

Consider the geometry depicted in Fig. 7(a). The domain D is the half-sphere of radius $\sqrt{n}$ centered at the origin, obtained by rotating the quarter-circle D' by the axis of symmetry. The field is measured on the surface of a sphere of radius $\sqrt{n}+\delta$ centered at the origin, obtained by rotating the half circumference M' of radius $\sqrt{n}+\delta$ by the axis of symmetry. As usual, by the uniqueness theorem it suffices to determine the field on this surface to characterize the field in the outside domain.

In this setting, a simple upper bound to N_0' is obtained by noticing that the integrand in (14) is at most 2 and that the length of M' is $O(\sqrt{n})$ as $n\to\infty$, so that

$$N_0'=O(\sqrt{n}),\quad \text{as } n\to\infty. \tag{19}$$

Substituting (19) into (17) and (18), we obtain

$$\begin{aligned}N_0^{\rm tot}&=O(n),\quad \text{as } n\to\infty,\\N_\epsilon(\mathcal{E})&=O(n(\log 1/\epsilon)^2),\quad \text{as } n\to\infty.\end{aligned}$$

D. Application to the Cylinder

Consider now the cylindrical geometry illustrated in Fig. 7(b), in which the domain D is the cylinder centered at the origin of radius $\sqrt{n}$ and height h, obtained by rotating the rectangle D' by the axis of symmetry. By the uniqueness theorem the field inside the outer annulus enclosed by the surface obtained rotating rectangle M' of length $\sqrt{n}$ and height h about the z axis, is determined by the field on the enclosing surface.[4]

To bound N_0' in this setting we decompose the integral in the left-hand side (LHS) of (14) into the sum of four terms, each one corresponding to a side of M'. Since M' has height h, the integral along each vertical side is at most $2h$ and, by symmetry, the integrals along the two horizontal sides are equal, so it suffices to study the integral over the domain $\{\mathbf{r}(s)=(s,0,h): s\in[0,\sqrt{n}]\}$. For any point $\mathbf{r}(s)$ in this domain, it is easy to see by elementary geometry that the extreme values of $\hat{R}\cdot\hat{t}$ are

[4]The edges of the rectangle are smoothed, so M' is analytic.

obtained at the two points r_1 and r_2 illustrated in Fig. 7(b), for which we have that $\hat{R}_1 \cdot \hat{t} = 1$, and $\hat{R}_2 \cdot \hat{t} = (1 + \frac{h^2}{(s+\delta)^2})^{-\frac{1}{2}}$. It follows that

$$\begin{aligned}\int_0^{\sqrt{n}} &\left(\max_{\mathbf{r}_d \in D'} \hat{R} \cdot \hat{t} - \min_{\mathbf{r}_d \in D'} \hat{R} \cdot \hat{t} \right) ds \\ &= \int_0^{\sqrt{n}} 1 - \left(1 + \frac{h^2}{(s+\delta)^2}\right)^{-\frac{1}{2}} ds \\ &\le \int_0^{\sqrt{n}} \frac{\frac{h^2}{(s+\delta)^2}}{\sqrt{1 + \frac{h^2}{(s+\delta)^2}}} ds \\ &= h \ \arctan \frac{h}{s+\delta} \bigg|_{\sqrt{n}}^{0} \\ &\le 2h \end{aligned} \tag{20}$$

where the inequality follows from $\sqrt{1+x^2} \le 1 + x^2$ for all x. Finally, substituting

$$N_0' \le 8h$$

into (17) and (18), we obtain

$$\begin{aligned} N_0^{\mathrm{tot}} &= O(h\sqrt{n}), \quad \text{as } n \to \infty, \\ N_\epsilon(\mathcal{E}) &= O\left(h\sqrt{n}(\log 1/\epsilon)^2\right), \quad \text{as } n \to \infty. \end{aligned}$$

VI. Concluding Remarks

This paper presented a physical approach to determining the number of d.o.f. available for communication in wireless interference networks. This corresponds to the number of independent channels available across any cut separating sources from destinations. It has been characterized, in arbitrary three-dimensional geometries, as an integral representing a variational measure of the difference vector between the sources' environment and the cut's surface. If such vector is highly variable in the sense of the defined integral measure, then the scattered field has a large information content in terms of number of available d.o.f.

The cut-set integral has then been computed in two canonical cases of interest. In these cases, it reduces to the wavelength-normalized geometric measure of the surface through which the information must flow.

We now wish to make some additional final remarks. The number of d.o.f. is a geometric measure which depends only on the physical environment surrounding the network. It is independent of the number of nodes forming the network. The number of nodes can then be chosen of smaller or equal order than the spatial resource represented by the cut-set integral to avoid information bottlenecks. For example, this is what happens in the half-sphere canonical configuration, where the number of nodes placed on the base of the half-sphere is of the same order of the cut-set surface.

The above point of view is also taken in the recent works [27], [28], where the authors argue that hierarchical cooperation schemes can be used with success in environments where the density of the nodes is small compared to the spatial resource available to them. In their model, however, the transmission power of the nodes must scale with the network's size to cope with increasing internode distances occurring at low node densities. When this is possible, the number of d.o.f. is not a bottleneck to cooperative schemes, and capacity results obtained exploiting signal diversity through hierarchical cooperation or interference alignment do not contradict the physical limits studied in this paper.

A final remark goes to the relationship between our results, the recent deterministic approach to wireless networks put forth by Avestimehr, Diggavi, and Tse [29], and the noisy network coding approach of Lim, Kim, El Gamal, and Chung [30]. These authors propose constructive schemes that are shown to be within a constant gap to the information-theoretic cut-set bound. This bound depends on the propagation channel and on the network topology, but this dependence is not explicitly modeled. Our approach takes the opposite point of view: rather than seeking novel coding schemes closer to the cut-set bound, we have focused on the physical limits of what the cut-set bound can be, and we have identified these limits by scaling the network's spatial dimension.

Appendix A
Proof of Theorem 4.2

As shown in [14], the (unordered) singular values for the geometry in the configuration depicted in Fig. 4(c) are

$$\begin{aligned}\sigma_k &= 2\pi \left\| h_k^{(2)}(2\pi(\sqrt{n}+\delta)) Y_{k,m}(\theta,\phi) \right\|_{\mathcal{E}} \\ &\quad \times \| j_k(2\pi\rho_d) Y_{k,m}(\theta_d,\phi_d) \|_{\mathcal{I}} \\ &= 2\pi \left| h_k^{(2)}(2\pi(\sqrt{n}+\delta)) \right| \\ &\quad \times \left(\int_D |j_k(2\pi\rho_d)\, Y_{k,m}(\theta_d,\phi_d)|^2 d\mathbf{r}_d \right)^{\frac{1}{2}} \end{aligned} \tag{21}$$

for $k = 0, 1, \ldots$, where $(\rho_d, \theta_d, \phi_d)$ is the representation of $\mathbf{r}_d \in D$ in a canonical spherical coordinate system, j_k is the spherical Bessel function of the first kind and order k, $h_k^{(2)}$ is the spherical Hankel function of second kind and order k, and $Y_{k,m}$ is the (kth, mth) spherical harmonic function.

The following technical lemma provides a uniform lower bound to the singular values up to $k \approx 2\pi\sqrt{n}$, and is needed to prove the theorem.

Lemma A.1: Let $0 < c_l < c_u < 1$. Then, for all $c_l 2\pi\sqrt{n} \le k \le c_u 2\pi\sqrt{n}$

$$\sigma_k = \Omega\left(\frac{1}{n^{1/4}}\right) \tag{22}$$

as $n \to \infty$.

Proof: It is convenient to rewrite the integral in (21) in terms of cylindrical Bessel functions of fractional order as follows:

$$\begin{aligned}\int_D |j_k(2\pi r_d)Y_{k,i}(\theta_d,\phi_d)|^2 dr_d &= \frac{1}{2}\int_0^{\sqrt{n}} |j_k(2\pi r_d)|^2 r_d^2 dr_d \\ &= \frac{1}{8}\int_0^{\sqrt{n}} |J_{\tilde{k}}(2\pi r_d)|^2 r_d dr_d \\ &= \frac{n}{16}\left[(J'_{\tilde{k}}(2\pi\sqrt{n}))^2 - \left(\frac{\tilde{k}^2}{4\pi^2 n} - 1\right)(J_{\tilde{k}}(2\pi\sqrt{n}))^2\right]\end{aligned} \tag{23}$$

where for notational convenience we defined $\tilde{k} \triangleq k + \frac{1}{2}$, and we used the normalization and symmetry properties of the harmonic functions in deriving the first equality; the second equality follows from [31, identity (10.1.1)]; finally, the third identity is obtained using [31, identity (5.54.2)] and the recurrence relations of Bessel functions [32, identity (9.1.27)]. Substituting (23) into (21) and rewriting the Hankel function in cylindrical coordinates, we obtain

$$\begin{aligned}\sigma_k = \frac{\pi n^{\frac{1}{2}}}{4(\sqrt{n}+\delta)^{\frac{1}{2}}}\left|H_{\tilde{k}}^{(2)}(2\pi(\sqrt{n}+\delta))\right| \Bigg[&(J'_{\tilde{k}}(2\pi\sqrt{n}))^2 \\ &- \left(\frac{\tilde{k}^2}{4\pi^2 n} - 1\right)(J_{\tilde{k}}(2\pi\sqrt{n}))^2\Bigg]^{\frac{1}{2}}\end{aligned} \tag{24}$$

where $J'_{\tilde{k}}(x)$ denotes the derivative of the Bessel function with respect to the argument x. In order to find a lower bound for σ_k we study the asymptotic behavior of the special functions appearing in the right-hand side (RHS) of (24).

We use Olver's uniform asymptotic expansions for Bessel functions [32, p. 368] and the corresponding error bounds [33] to obtain that, as $n \to \infty$

$$\left|H_{\tilde{k}}^{(2)}(\tilde{k}z_\delta)\right| = \Omega\left(\frac{2}{\tilde{k}^{\frac{1}{3}}}\left(\frac{4\zeta_\delta}{1-z_\delta^2}\right)^{\frac{1}{4}}\left|\mathrm{Ai}\left(e^{-i\frac{2}{3}\pi}\tilde{k}^{\frac{2}{3}}\zeta_\delta\right)\right|\right) \tag{25}$$

$$J_{\tilde{k}}(\tilde{k}z) = \Omega\left(\left(\frac{4\zeta}{1-z^2}\right)^{\frac{1}{4}}\frac{\mathrm{Ai}(\tilde{k}^{\frac{2}{3}}\zeta)}{\tilde{k}^{\frac{1}{3}}}\right) \tag{26}$$

$$J'_{\tilde{k}}(\tilde{k}z) = \Omega\left(-\frac{2}{z}\left(\frac{1-z^2}{4\zeta}\right)^{\frac{1}{4}}\frac{\mathrm{Ai}'(\tilde{k}^{\frac{2}{3}}\zeta)}{\tilde{k}^{\frac{2}{3}}}\right) \tag{27}$$

wherein the constants only depend on c_l, c_u and δ; $\mathrm{Ai}(\cdot)$ and $\mathrm{Ai}'(\cdot)$ denote the Airy function of the first kind and its derivative with respect to the argument; $z \triangleq \frac{2\pi\sqrt{n}}{\tilde{k}} \in [\frac{1}{c_u}, \frac{1}{c_l}]$ denotes the ratio between the argument and the index in the Bessel functions; $z_\delta \triangleq \frac{2\pi(\sqrt{n}+\delta)}{\tilde{k}} = z + \frac{2\pi\delta}{\tilde{k}}$ denotes the same ratio for the Hankel function. The function $\zeta \triangleq \zeta(z)$ is defined as $\frac{2}{3}(-\zeta(z))^{3/2} = \int_1^z \frac{\sqrt{u^2-1}}{u}du, \quad z \geq 1$, and is negative for all $z > 1$. Similarly, we define $\zeta_\delta \triangleq \zeta(z_\delta)$. Notice that ζ and ζ_δ are bounded, since by assumption $0 < c_l < c_u < 1$.

Next, we study the asymptotic behavior of $\mathrm{Ai}(\cdot)$ and $\mathrm{Ai}'(\cdot)$. Observe that the argument of the Airy function in (25) is complex valued, and it has phase $-\frac{5}{3}\pi$, as $\zeta_\delta < 0$. Thus, we use the asymptotic expansions for the Airy functions *off* the negative real axis [32, 10.4.59], and the corresponding bound on the error term [34, p. 116], to obtain that, as $n \to \infty$

$$\begin{aligned}\left|\mathrm{Ai}\left(e^{-i\frac{2}{3}\pi}\tilde{k}^{\frac{2}{3}}\zeta_\delta\right)\right| &= \Omega\left(\left|\frac{e^{-\frac{2}{3}\left(e^{-i\frac{2}{3}\pi}\tilde{k}^{\frac{2}{3}}\zeta_\delta\right)^{3/2}}}{\left(e^{-i\frac{2}{3}\pi}\tilde{k}^{\frac{2}{3}}\zeta_\delta\right)^{\frac{1}{4}}}\right|\right) \\ &= \Omega\left(\left|\left(\tilde{k}^{\frac{2}{3}}\zeta_\delta\right)^{-\frac{1}{4}}\right|\right).\end{aligned} \tag{28}$$

where the constants only depend on c_l, c_u and δ. Similarly, as $\zeta < 0$ for $z > 1$, the asymptotic expansions for the Airy functions *on* the negative real axis [32, 10.4.62] and [34, p. 394] yield

$$\mathrm{Ai}\left(\tilde{k}^{\frac{2}{3}}\zeta\right) = \Omega\left((-\tilde{k}^{\frac{2}{3}}\zeta)^{-\frac{1}{4}}\sin\left(\frac{2}{3}\tilde{k}(-\zeta)^{3/2} + \frac{\pi}{4}\right)\right) \tag{29}$$

$$\mathrm{Ai}'\left(\tilde{k}^{\frac{2}{3}}\zeta\right) = \Omega\left((-\tilde{k}^{\frac{2}{3}}\zeta)^{\frac{1}{4}}\cos\left(\frac{2}{3}\tilde{k}(-\zeta)^{3/2} + \frac{\pi}{4}\right)\right) \tag{30}$$

as $n \to \infty$.

Substituting (28), (29), and (30) into (25), (26), and (27), using (24) and the fact that $\frac{\zeta_\delta(1-z^2)}{\zeta(1-z_\delta^2)} = \Omega(1)$ as $n \to \infty$, we obtain that, for all $c_l 2\pi\sqrt{n} \leq k \leq c_u 2\pi\sqrt{n}$

$$\begin{aligned}\sigma_k &= \Omega\Bigg(\frac{n^{\frac{1}{4}}}{\tilde{k}}\frac{1}{z}\Bigg[\cos^2\left(\frac{2}{3}\tilde{k}(-\zeta)^{3/2} + \frac{\pi}{4}\right) \\ &\qquad + (z^2-1)\sin^2\left(\frac{2}{3}\tilde{k}(-\zeta)^{3/2} + \frac{\pi}{4}\right)\Bigg]^{\frac{1}{2}}\Bigg) \\ &= \Omega\left(\frac{1}{n^{\frac{1}{4}}}\left[1 + (z^2-2)\sin^2\left(\frac{2}{3}\tilde{k}(-\zeta)^{3/2} + \frac{\pi}{4}\right)\right]^{\frac{1}{2}}\right) \\ &= \Omega\left(\frac{1}{n^{\frac{1}{4}}}\right), \quad \text{as } n \to \infty\end{aligned} \tag{31}$$

where we used $z = \frac{2\pi\sqrt{n}}{\tilde{k}}$ in deriving the second equality, and the fact that the term in square brackets is uniformly bounded away from zero for all $z \geq \frac{1}{c_u} > 1$. ■

At this point we can provide a proof for Theorem 4.2.

Proof: The proof shows that, given any subspace $\mathcal{A}' \subseteq \mathcal{A}$ of dimension $\Omega(n)$ as $n \to \infty$, there exists a current density $I \in \mathcal{I}$ whose corresponding magnetic vector potentials A cannot be approximated in $\mathcal{A}'$ with constant error as $n \to \infty$.

By Theorem 4.1, it suffices to consider subspaces generated by the left singular functions of the Green function operator.

Thus, let $0 < c_l < c_u < 1$ and consider the subspace $\mathcal{A}'$ generated by left singular functions associated to the $(c_u - c_l)n$ largest singular values. For n large enough, it is always possible to find an index $k \in [2\pi c_l\sqrt{n}, \leq 2\pi c_u\sqrt{n}]$ such that the kth left singular function orthogonal to $\mathcal{A}'$. Consider the input current density

$$I(\mathbf{r}_d) = ||I||_{\mathcal{I}} v_k(\mathbf{r}_d), \quad \mathbf{r}_d \in D$$

for such index k. The corresponding magnetic vector potential is

$$A(\mathbf{r}) = GI(\mathbf{r}_d) = ||I||_{\mathcal{I}} u_k(\mathbf{r}_d), \quad \mathbf{r} \in V.$$

Since u_k is orthogonal to $\mathcal{A}'$, the squared error in approximating $A(\mathbf{r})$ with its orthogonal projecting on $\mathcal{A}'$ is equal to the norm of $A(\mathbf{r})$. On the other hand, the power constraint (4) and Lemma A.1 yield

$$||A(\mathbf{r})||^2 = ||I||^2_{\mathcal{I}} |\sigma_k|^2 \geq \sqrt{n}P.$$

Thus, taking the limit as $n \to \infty$, it follows that the error in approximating A in $\mathcal{A}'$ tends to infinity, so A cannot be approximated in $\mathcal{A}'$. ■

REFERENCES

[1] P. Gupta and P. R. Kumar, "The capacity of wireless networks," *IEEE Trans. Inf. Theory*, vol. 42, no. 2, pp. 388–404, Mar. 2000.

[2] M. Franceschetti, O. Dousse, D. N. C. Tse, and P. Thiran, "Closing the gap in the capacity of wireless networks via percolation theory," *IEEE Trans. Inf. Theory*, vol. 53, no. 3, pp. 1009–1018, Mar. 2007.

[3] S. R. Kulkarni and P. Viswanath, "A deterministic approach to throughput scaling in wireless networks," *IEEE Trans. Inf. Theory*, vol. 50, no. 11, pp. 1041–1049, Jun. 2004.

[4] Y. Nebat, R. Cruz, and S. Bhardwaj, "The capacity of wireless networks in nonergodic random fading," *IEEE Trans. Inf. Theory*, vol. 55, no. 6, pp. 2478–2493, Jun. 2009.

[5] F. Xue, L.-L. Xie, and P. R. Kumar, "The transport capacity of wireless networks over fading channels," *IEEE Trans. Inf. Theory*, vol. 51, no. 3, pp. 834–847, Mar. 2005.

[6] A. Özgür, O. Lévêque, and D. N. C. Tse, "Hierarchical cooperation achieves optimal capacity scaling in ad hoc networks," *IEEE Trans. Inf. Theory*, vol. 53, no. 10, pp. 3549–3572, Oct. 2007.

[7] S. Aeron and V. Saligrama, "Wireless ad hoc networks: Strategies and scaling laws for the fixed SNR regime," *IEEE Trans. Inf. Theory*, vol. 53, no. 6, pp. 2044–2059, Jun. 2007.

[8] J. Ghaderi, L.-L. Xie, and X. Shen, "Hierarchical cooperation in ad hoc networks: Optimal clustering and achievable throughput," *IEEE Trans. Inf. Theory*, vol. 55, no. 8, pp. 3425–3436, Aug. 2009.

[9] L.-L. Xie, "On information-theoretic scaling laws for wireless networks," *IEEE Trans. Inf. Theory*, submitted for publication.

[10] V. R. Cadambe and S. A. Jafar, "Interference alignment and degrees of freedom of the k-user interference channel," *IEEE Trans. Inf. Theory*, vol. 54, no. 8, pp. 3425–3441, Aug. 2008.

[11] M. A. Maddah-Ali, S. A. Motahari, and A. K. Khandani, "Communication over MIMO X channels: Interference alignment, decomposition, and performance analysis," *IEEE Trans. Inf. Theory*, vol. 54, no. 8, pp. 3457–3470, Aug. 2008.

[12] A. Özgür and D. N. C. Tse, "Achieving linear scaling with interference alignment," in *Proc. IEEE International Symp. Inf. Theory*, Seoul, Korea, Jul. 2009.

[13] A. El Gamal and Y.-H. Kim, "Lecture notes on network information theory," 2010 [Online]. Available: http://arxiv.org/abs/1001.3404

[14] M. Franceschetti, M. D. Migliore, and P. Minero, "The capacity of wireless networks: information-theoretic and physical limits," *IEEE Trans. Inf. Theory*, vol. 55, no. 8, pp. 3413–3424, Aug. 2009.

[15] M. Franceschetti, M. D. Migliore, P. Minero, and F. Schettino, "The degrees of freedom of wireless networks," in *Proc. 2009 Int. Conf. Electromagn. Adv. Applicat.*, Torino, Italy, Sep. 2009.

[16] O. M. Bucci and G. Franceschetti, "On the spatial bandwidth of scattered fields," *IEEE Trans. Antennas Propag.*, vol. 35, no. 12, pp. 1445–1455, Dec. 1987.

[17] O. M. Bucci and G. Franceschetti, "On the degrees of freedom of scattered fields," *IEEE Trans. Antennas Propag.*, vol. 37, no. 7, pp. 918–926, Jul. 1989.

[18] O. M. Bucci, C. Gennarelli, and C. Savarese, "Representation of electromagnetic fields over arbitrary surfaces by a finite and non redundant number of samples," *IEEE Trans. Antennas Propag.*, vol. 46, no. 3, pp. 351–359, Mar. 1998.

[19] D. Slepian, "On bandwidth," *Proc. IEEE*, vol. 64, no. 3, Mar. 1976.

[20] M. D. Migliore, "On electromagnetics and information theory," *IEEE Trans. Antennas Propag.*, vol. 56, no. 10, pp. 3188–3200, Oct. 2010.

[21] M. D. Migliore, "On the role of the number of degrees of freedom of the field in MIMO channels," *IEEE Trans. Antennas Propag.*, vol. 54, no. 2, pp. 620–628, Feb. 2006.

[22] A. Pinkus*, n-Widths in Approximation Theory*. New York: Springer-Verlag, 1985.

[23] F. K. Gruber and E. A. Marengo, "New aspects of electromagnetic information theory for wireless and antenna systems," *IEEE Trans. Antennas Propag.*, vol. 56, no. 11, pp. 3470–3484, Nov. 2008.

[24] D. Slepian, "Some comments on Fourier analysis, uncertainty and modeling," *SIAM Rev.*, vol. 25, no. 3, pp. 379–393, Jul. 1983.

[25] R. Caccioppoli, "Sulla quadratura delle superfici piane e curve," (in Italian) *Rend. Acc. Naz. Lincei*, vol. 6, no. 6, pp. 142–146, 1927.

[26] J. A. Stratton*, Electromagnetic Theory*. New York: Mc Graw-Hill, 1941.

[27] A. Özgür, R. Johari, D. N. C. Tse, and O. Lévêque, "Information theoretic operating regimes of large wireless networks," *IEEE Trans. Inf. Theory*, vol. 56, no. 1, pp. 427–437, Jan. 2010.

[28] A. Özgür, O. Lévêque, and D. N. C. Tse, "Linear capacity scaling in wireless networks: Beyond physical limits?," in *Proc. IEEE Inf. Theory Applicat. Workshop*, San Diego, CA, Feb. 2010.

[29] S. Avestimehr, S. Diggavi, and D. N. C. Tse, "A deterministic approach to wireless relay networks," *IEEE Trans. Inf. Theory* [Online]. Available: http://arxiv.org/abs/0710.3781

[30] S. H. Lim, Y. Kim, A. El Gamal, and S. Chung, "Noisy network coding," [Online]. Available: http://arxiv.org/pdf/1002.3188v2

[31] I. S. Gradshteyn and I. M. Ryzhik, *Tables of Integrals, Series, and Products*, A. Jeffrey, Ed. New York: Academic, 1994.

[32] M. Abramowitz and I. A. Stegun*, Handbook of Mathematical Functions With Formulas, Graphs, and Mathematical Tables*, 9th ed. New York: Dover, 1972.

[33] F. W. J. Olver, "The asymptotic expansion of Bessel functions of large order," *Philos. Trans. Roy. Soc. London Ser. A*, vol. 247, pp. 328–368, 1954.

[34] F. W. J. Olver, "Asymptotics and special functions, (reprint)," in *AKP Classics*. Wellesley, MA: A. K. Peters, 1997.

Massimo Franceschetti (M'98) received the Laurea degree (*magna cum laude*) in computer engineering from the University of Naples "Federico II", Naples, Italy, in 1997, and the M.S. and Ph.D. degrees in electrical engineering from the California Institute of Technology (Caltech), Pasadena, in 1999, and 2003, respectively.

He is an Associate Professor with the Department of Electrical and Computer Engineering, University of California at San Diego (UCSD). Before joining UCSD, he was a Postdoctoral Scholar with the University of California at Berkeley for two years. He has held visiting positions with the Vrije Universiteit Amsterdam, the Ecole Polytechnique Federale de Lausanne, and the University of Trento. His research interests are in communication systems theory and include random networks, wave propagation in random media, wireless communication, and control over networks.

Dr. Franceschetti is an Associate Editor for Communication Networks of the IEEE TRANSACTIONS ON INFORMATION THEORY (2009–2012) and has served as Guest Editor for two issues of the IEEE JOURNAL ON SELECTED AREAS IN COMMUNICATIONS. He was awarded the C. H. Wilts Prize in 2003 for Best Doctoral Thesis in electrical engineering at Caltech; the S. A. Schelkunoff Award in 2005 for Best Paper in the IEEE TRANSACTIONS ON ANTENNAS AND PROPAGATION; a National Science Foundation (NSF) CAREER award in 2006, an ONR Young Investigator Award in 2007; and the IEEE Communications Society Best Tutorial Paper Award in 2010.

Marco Donald Migliore (M'04) received the Laurea degree (with highest honors) in electronic engineering and the Ph.D. degree in electronics and computer science from the University of Napoli "Federico II", Naples, Italy, in 1990 and 1994, respectively.

He is currently an Associate Professor with the University of Cassino, Cassino, Italy, where he teaches adaptive antennas, radio propagation in urban areas, and electromagnetic fields. He has also been appointed Professor at the University of Napoli "Federico II", where he teaches microwaves. In the past, he taught antennas and propagation at the University of Cassino and microwave measurements at the University of Napoli "Federico II". He is also a consultant to industries in the field of advanced antenna measurement systems. His main research interests are antenna measurement techniques, adaptive antennas, MIMO antennas and propagation, and medical and industrial applications of microwaves.

Dr. Migliore is a Member of the Antenna Measurements Techniques Association (AMTA), the Italian Electromagnetic Society (SIEM), the National Inter-University Consortium for Telecommunication (CNIT), and the Electromagnetics Academy. He is listed in Marquis *Who's Who in the World*, *Who's Who in Science and Engineering*, and in *Who's Who in Electromagnetics*.

Paolo Minero (S'05–M'11) received the Laurea degree (with highest honors) in electrical engineering from the Politecnico di Torino, Torino, Italy, in 2003, the M.S. degree in electrical engineering from the University of California at Berkeley in 2006, and the Ph.D. degree in electrical engineering from the University of California at San Diego in 2010.

He is an Assistant Professor with the Department of Electrical Engineering, University of Notre Dame, Notre Dame, IN. Before joining the University of Notre Dame, he was a Postdoctoral Scholar with the University of California at San Diego for six months. His research interests are in communication systems theory and include information theory, wireless communication, and control over networks.

Dr. Minero received the U.S. Vodafone Fellowship in 2004 and 2005, and the Shannon Memorial Fellowship in 2008.

Fulvio Schettino (M'02) received the Laurea degree (cum laude) in electrical engineering and the Ph.D degree in 2001, both from the University of Naples, Naples, Italy.

Since 2001, he has been an Assistant Professor in the Department of Electrical Engineering, University of Cassino, Cassino, Italy. His research interests include analytical and numerical techniques for antenna and circuits analysis and design and adaptive antennas design.

Dr. Schettino received the Giorgio Barzilai Prize for the Best Young Scientist paper at the Italian National Congress on Electromagnetics in 2006.